Journal of Analytical Science and Technology

RESEARCH ARTICLE Open Access

Multi-omics analysis of aniline-degrading bacterium, *Delftia* sp. K82

Sang-Yeop Lee[1†], Sung Ho Yun[2†], Hayoung Lee[1,3], Giwan Seo[1] and Seung Il Kim[1,3*]

Abstract

Delftia sp. K82 is a soil bacterium capable of utilizing monocyclic aromatic hydrocarbons, including aniline, as its sole carbon and nitrogen source. In this study, the genome analysis of *Delftia* sp. K82 was completed and the genome data (6117 protein-coding genes and 62 RNA genes) were utilized for proteomic and transcriptomic analysis of *Delftia* sp. K82 cultured in aniline culture medium. Using these multi-omics approaches (genomics, transcriptomics, and proteomics), complete gene clusters for aniline biodegradation pathways were identified and transcriptomic or proteomic sets specifically induced in aniline culture conditions were elucidated. These data provide multi-layered information on the metabolic characteristics of *Delftia* sp. K82. The findings suggest that multi-omics approaches are useful analytical tools for the elucidation of the metabolic diversity of soil bacteria and for the identification of novel metabolic enzymes.

Keywords: *Delftia* sp. K82, Genomics, Transcriptomics, Proteomics, Biodegradation, Aniline

Introduction

Delftia sp. K82 was isolated from soil in the Gyeonggi province of Korea in 1992. *Delftia* sp. K82 has been previously known as *Pseudomonas* sp. K82 (Yun et al. 2004). This strain degrades monocyclic aromatic hydrocarbons (MAHs), such as aniline analogs (aniline, 3-methyl aniline, and 4-methyl-aniline) and benzoate analogs (benzoate and *p*-hydroxybenzoate), as the sole carbon or nitrogen source (Yun et al. 2004).

Aniline and its analogs are toxic organic compounds and important environmental pollutants (Feng et al. 2020; Liu et al. 2002). In general, major dioxygenases for aniline (aniline analogs) biodegradation are categorized as intradiol cleavage enzymes (catechol 1,2-dioxygenase) or extradiol cleavage enzymes (catechol 2,3-dioxygenase) (Lee et al. 2016). The two types of catechol dioxygenases lead to different biodegradation pathways (Fuchs et al. 2011).

Delftia sp. K82 degrades MAHs using both types of catechol dioxygenases, and its biodegradation activity has been confirmed using two dimensional-gel-based proteomic analysis (Yun et al. 2004). In this strain, aniline-induced catechol 2,3-dioxygenase and other enzymes of the extradiol cleavage pathway as the major biodegradation pathway. Additionally, catechol 1,2-dioxygenase activities have been detected (Yun et al. 2004). However, previous gel-based proteomic analyses have not revealed enough information on the biodegradation pathway to fully understand the metabolic activities of *Delftia* sp. K82 (Yun et al. 2004).

Therefore, in this study, whole genome sequencing was performed to comprehensively understand the genomic characteristics for aniline biodegradation. Next, RNA sequencing (RNA-Seq) and liquid chromatography–tandem mass spectrometry (LC-MS/MS)-based proteomic analysis were performed to obtain multi-layered information on aniline biodegradation activities. This omics approach determined the global response of *Delftia* sp. K82 to aniline culture conditions and provided complete information on the aniline

* Correspondence: ksi@kbsi.re.kr
†Sang-Yeop Lee and Sung Ho Yun contributed equally to this work.
[1]Research Center for Bioconvergence Analysis, Korea Basic Science Institute, Ochang 28119, South Korea
[3]Department of Bio-Analytical Science, University of Science and Technology (UST), Daejeon 34113, Korea
Full list of author information is available at the end of the article

Table 1 Genomic feature of *Delftia* sp. K82

Attribute	Value	% of Total
Genome size (bp)	7,112,516	100
DNA coding (bp)	6,251,083	87.9
DNA G+C (bp)	4,667,030	65.9
DNA scaffolds	21	n/a
Total genes	6327	100
Protein coding genes	6117	96.7
RNA genes	62	1.0
Pseudo genes	148	2.3
Genes in internal clusters	723	11.4
Genes with function prediction	4386	69.3
Genes assigned to COGs	4104	64.9
Genes with Pfam domains	4390	69.4
Genes with signal peptides	1272	20.1
Genes with transmembrane helices	1391	21.9
CRISPR repeats	0	0

biodegradation pathway. From this study, it was confirmed that *Delftia* sp. K82 induced two aniline degradation pathways, even though the extradiol pathway plays a major role. Other metabolic characteristics induced by aniline were also elucidated using these approaches.

In this study, it was demonstrated that multi-omics analysis is a valuable tool for the elucidation of unknown or hidden metabolic diversity of soil bacteria.

Experimental

Bacterial cultivation and genomic DNA preparation

Delftia sp. K82 was isolated as previously described (Yun et al. 2004). For extraction of genomic DNA, RNA, and proteome, *Delftia* sp. K82 was grown in Luria-Bertani (LB) broth at 30 °C until later part of an exponential phase that an optical density at 600 nm (OD_{600}) of 0.7~0.8. Extraction and purification of genomic DNA was performed using a G-spin DNA extraction kit (iNtRON Biotechnology Inc., Sungnam, Korea), according to the manufacturer's instructions. *Delftia* sp. K82 cultured in aniline media was prepared as previously described (Yun et al. 2004). Briefly, aniline media was composed of potassium phosphate buffer (pH 6.25) containing 3.4 mM $MgSO_4$, 0.3 mM $FeSO_4$, 0.2 mM $CaCO_3$, l0 mM NH_4Cl, and 5 mM aniline.

Table 2 Number of differentially expressed genes and proteins according omics-analysis of *Delftia* sp. K82

DEP(ANI/LB)	No. of proteins
Aniline only	472
l2fc* ≥ 1	299
1 ≥ l2fc ≤ − 1	1549
l2fc ≤ − 1	438
LB only	409
DEG(ANI/LB)	No. of genes
l2fc ≥ 1 and p value < 0.05	1262
l2fc ≤ − 1 and p value < 0.05	2657
DEP and DEG	No. of proteins and genes
Upregulate	195
Downregulate	442

*log2 fold change

Genome sequencing and assembly

The *Delftia* sp. K82 genome was sequenced on an Illumina MiSeq platform (Illumina, San Diego, CA, USA) using a paired-end and a mate-pair strategy. Paired-end and mate-pair libraries were created with insert sizes of 250–350 bp and 5 kb, respectively. Low-quality reads were trimmed using PRINSEQ lite (Schmieder and Edwards 2011). De-novo assembly and construction of the draft genome of *Delftia* sp. K82 was performed with 41,757,452 high-quality reads using CLC Genomics Workbench v7.0 (QIAGEN Bioinformatics, Germantown, MD, USA).

Genome annotation

Genome annotation was performed using Prokka 2.6.0, with the *Delftia* genus protein database downloaded from Uniprot and the Rapid Annotation using Subsystem Technology (RAST) annotation server (Seemann 2014; Aziz et al. 2008). Pairwise comparisons were performed for validation of predicted open reading frames. The rRNA and tRNA genes were detected using RNAmmer and tRNAscan-SE, respectively (Lagesen et al. 2007; Chan and Lowe 2019). Genes in internal clusters were identified using BLASTclust with thresholds of > 70% coverage length and > 30% sequence identity. Transmembrane helices, signal peptides, and clustered regularly interspaced short palindromic repeats (CRISPR) were analyzed using TMHMM, signalP, and CRISPRfinder, respectively (Chen et al. 2003; Almagro Armenteros et al. 2019; Grissa et al. 2007).

LC-MS/MS analysis (proteomic analysis)

To extract total protein samples, harvested bacteria were boiled in 10% sodium dodecyl sulfate (SDS) for 10 min, and the supernatant was obtained by centrifugation (15,000×g for 10 min). Extracted proteins were then fractionated using 12% SDS-polyacrylamide gel electrophoresis. Tryptic digestion was performed, as previously described (Yun et al. 2011b). Tryptic peptides were dissolved with 0.5% trifluoroacetic acid prior to further analysis. Concentrated tryptic peptides were directed onto a 10 cm × 75 μm ID C18 reverse-phase column at a flow rate of 300 nL/min and were eluted with a gradient of

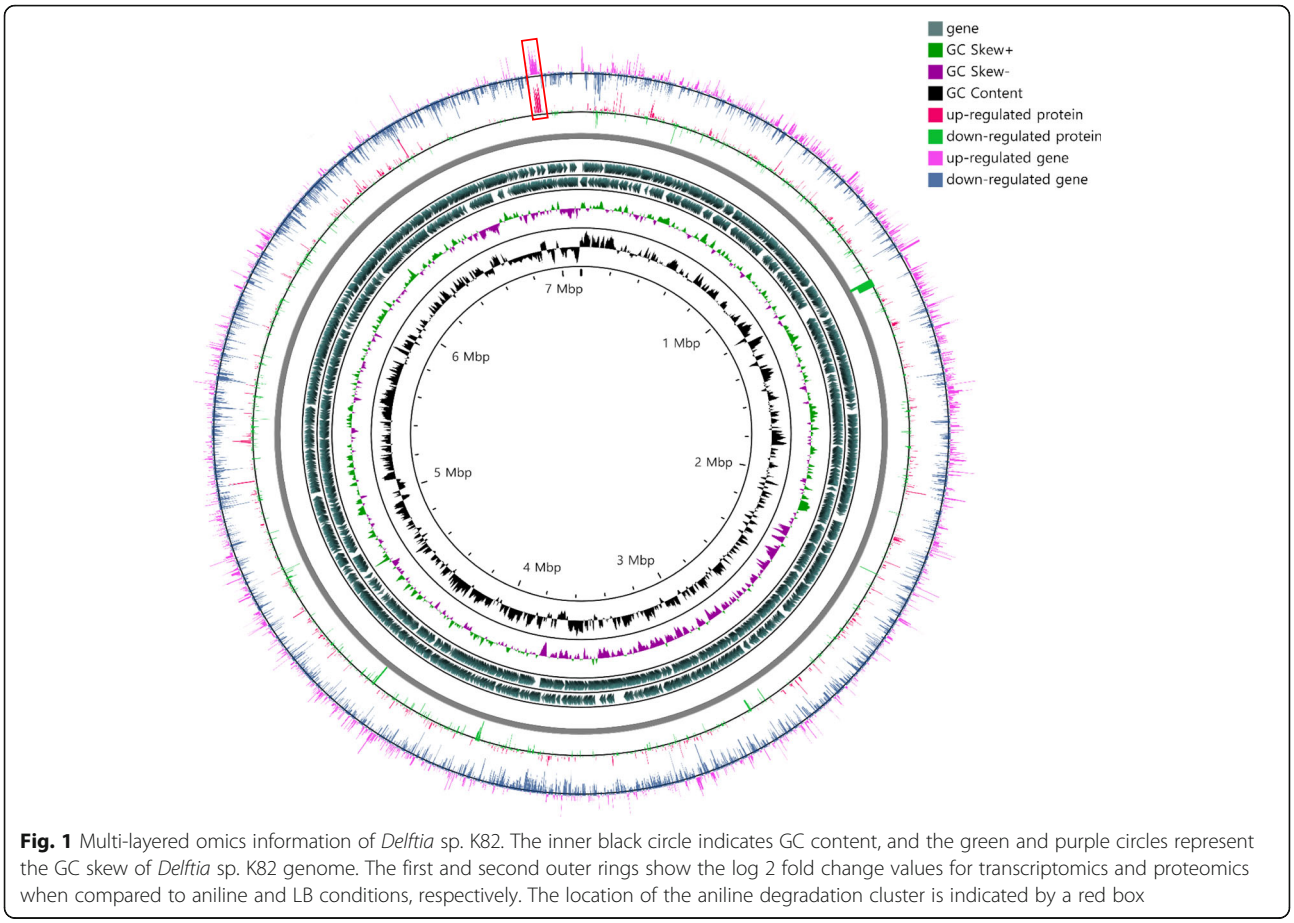

Fig. 1 Multi-layered omics information of *Delftia* sp. K82. The inner black circle indicates GC content, and the green and purple circles represent the GC skew of *Delftia* sp. K82 genome. The first and second outer rings show the log 2 fold change values for transcriptomics and proteomics when compared to aniline and LB conditions, respectively. The location of the aniline degradation cluster is indicated by a red box

8–55% acetonitrile over 80 min. All MS and MS/MS spectra were acquired on an LTQ-Velos electrospray ionization ion trap mass spectrometer (Thermo Scientific, Waltham, MA, USA) in data-dependent mode. MASCOT (v.2.4) was used for protein identification. To quantitatively compare the protein abundance in each sample, differentially expressed proteins (DEPs) were calculated using the mol% value.

RNA-Seq and bioinformatics analysis

RNA isolation was performed using the RNeasy Plus Mini Kit (QIAGEN, Valencia, CA, USA), and RNA quality was confirmed using the Agilent RNA 6000 Nano kit (Agilent Technologies, Santa Clara, CA, USA). Magnetic beads conjugated to oligo (dT) were used to enrich poly (A) mRNA before cDNA library construction. The final library sizes and qualities were evaluated electrophoretically using an Agilent High Sensitivity DNA kit (Agilent Technologies). Subsequently, the library was sequenced on an Illumina NovaSeq6000 sequencer (Illumina, San Diego, CA, USA). Low-quality reads and adapter sequences were filtered out using Trimmomatic (v.0.32) (Bolger et al. 2014). Filtered reads were aligned to the *Delftia* sp. K82 genome (Accession: NZ_MYFL00000000.1) using STAR (v.2.3.0) (Dobin et al. 2013). The number of mapped sequences on genes was calculated using HTSeq-count (v.0.5.4) (Anders et al. 2015), and differentially expressed genes (DEGs) were identified using the R package DESeq2 (Love et al. 2014). Functional annotation of DEGs were analyzed using GSEA-Pro v.3 (http://gseapro.molgenrug.nl/), and the CGView server was used to construct the circular map (Grant and Stothard 2008).

Results and discussion

Summary of genomic, transcriptomic, and proteomic analyses

The genome of *Delftia* sp. K82 consisted of 21 scaffolds, and the total length of the scaffolds was 7,112,516 bp, with an average GC content of 65.9%. *Delftia* sp. K82 had 6327 genes. Among them, 6117 genes (96.7%) were protein-coding genes. A total of 4104 genes of the protein-coding sequence (64.9%) were assigned to Clusters of Orthologous Group categories and 4386 (69.3%) were annotated as putative proteins. Genome data were deposited in the National Center for Biotechnology Information (NZ_MYFL00000000.1). Table 1 provides a more detailed summary of the genome properties.

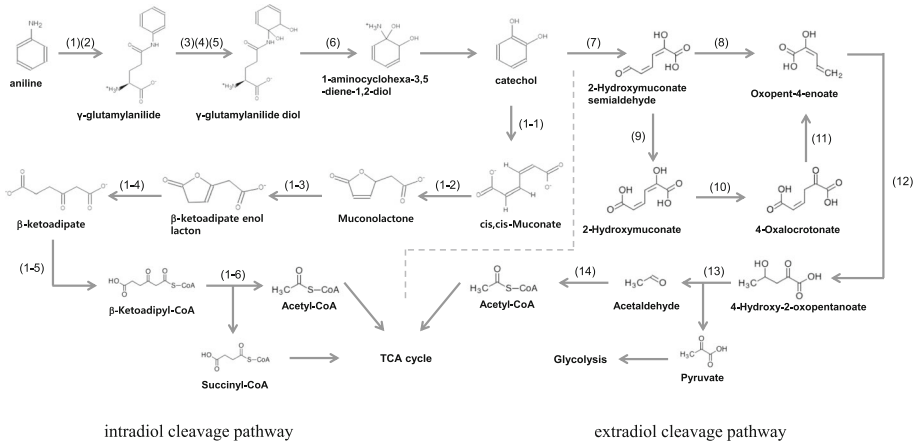

Fig. 2 Two metabolic pathway of aniline degradation in *Delftia* sp. K82. Two metabolic pathways (an intradiol cleavage pathway and an extradiol cleavage pathway) of aniline degradation in *Delftia* sp. K82 have been identified. Enzymes of each pathway are numbered and are listed in Table 3. The aniline oxygenase complex of *Delftia* sp. K82 is composed of six enzymes (Nos. 1~6) and four reaction steps for the conversion of aniline into catechol. The locus_tag and enzyme name of each number are as follows: No.1, KDK82_RS31140, glutamine synthetase; No.2,KDK82_RS31135,glutamine amidotransferase ; No.3,KDK82_RS31130,Large subunit of dioxygenase; No.4,KDK82_RS31125,small subunit of dioxygenase ; No.5,KDK82_RS31120,aniline dioxygenase reductase; No.6,KDK82_RS31110,small ferredoxin-like protein ; No.7,KDK82_RS31105, catechol 2,3-dioxygenase; No.8,KDK82_RS31090, 2-hydroxymuconic semialdehyde hydrolase; No.9, KDK82_RS31095, 2-hydroxymuconic semialdehyde dehydrogenase; No.10, KDK82_RS31050, 4-oxalocrotonate tautomerase family protein; No.11, KDK82_RS31080, 2-oxo-3-hexenedioate decarboxylase; No.12, KDK82_RS31085, 2-oxopent-4-enoate hydratase; No.13, KDK82_RS31060, 4-hydroxy-2-oxovalerate aldolase; No.14, KDK82_RS31065, acetaldehyde dehydrogenase; No.1-1, KDK82_RS22950, catechol 1,2-dioxygenase; No.1-2, KDK82_RS22965, mandelate racemase; No.1-3,KDK82_RS22960, muconolactone delta-isomerase; No.1-4, KDK82_RS23310, 3-oxoadipate enol-lactonase; No.1-5, KDK82_RS01060, 3-oxoadipate CoA-transferase; No.1–6, KDK82_RS17030, acetyl-CoA C-acyltransferase

Table 3 Results of multi-omics analysis of aniline degradation pathway in *Delftia* sp. K82

Index	Locus_tag	Product	log2 Fold change (ANI/LB)	
			Transcriptome	Proteome
1	KDK82_RS31140	Glutamine synthetase	3.631	7.356
2	KDK82_RS31135	Glutamine amidotransferase	3.129	4.650
3	KDK82_RS31130	Large subunit of dioxygenase	3.492	8.566
4	KDK82_RS31125	Small subunit of dioxygenase	2.907	3.552
5	KDK82_RS31120	Aniline dioxygenase reductase	4.322	6.663
6	KDK82_RS31110	Small ferredoxin-like protein	1.322	ANI only
7	KDK82_RS31105	Catechol 2,3-dioxygenase	6.809	5.952
8	KDK82_RS31090	2-Hydroxymuconic semialdehyde hydrolase	3.907	7.057
9	KDK82_RS31095	2-Hydroxymuconic semialdehyde dehydrogenase	5.229	5.356
10	KDK82_RS31050	4-Oxalocrotonate tautomerase family protein	6.229	6.584
11	KDK82_RS31080	2-Oxo-3-hexenedioate decarboxylase	5.322	6.466
12	KDK82_RS31085	2-Oxopent-4-enoate hydratase	4.269	4.831
13	KDK82_RS31060	4-Hydroxy-2-oxovalerate aldolase	8.492	7.649
14	KDK82_RS31065	Acetaldehyde dehydrogenase	6.662	6.733
1-1	KDK82_RS22950	Catechol 1,2-dioxygenase	1.100	4.427
1-2	KDK82_RS22965	Mandelate racemase	0.907	ANI only
1-3	KDK82_RS22960	Muconolactone delta-isomerase	− 1.121	0.942
1-4	KDK82_RS23310	3-Oxoadipate enol-lactonase	− 3.121	− 0.199
1-5	KDK82_RS01060	3-Oxoadipate CoA-transferase	− 3.059	ANI only
1-6	KDK82_RS17030	Acetyl-CoA C-acyltransferase	− 0.858	ANI only

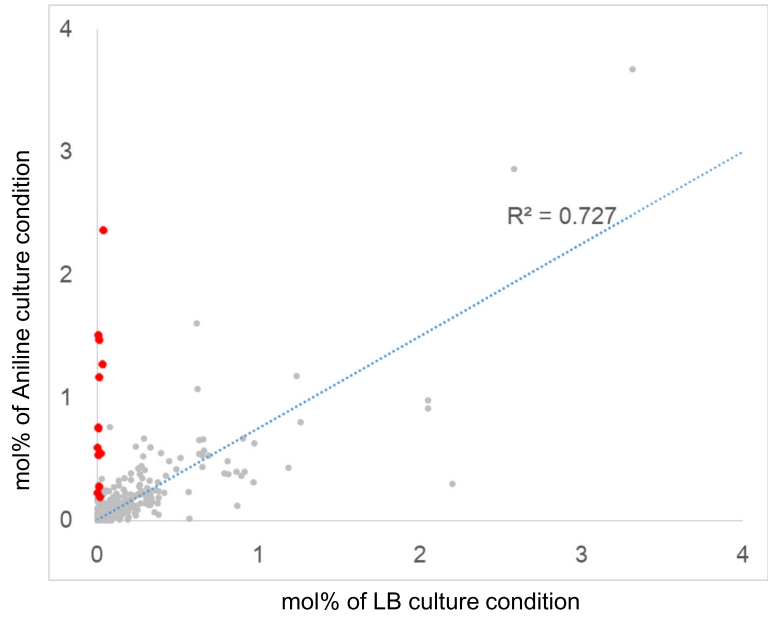

Fig. 3 Correlation of two proteome sets of *Delftia* sp. K82. The two proteome sets are highly correlated (R^2: 0.727) when aniline degradation cluster proteins are excluded. Red dots indicate aniline-degrading cluster proteins. However, when aniline degradation-related proteins are included, r squared value of two proteome sets was decreased to 0.519

For RNA-Seq and proteomic analysis using LC/MS-MS analysis, two cultures (LB media and aniline media) of *Delftia* sp. K82 were prepared, according to a previously described procedure (Yun et al. 2004). The results of transcriptomic and proteomic analyses are summarized in Table 2. A total of 3919 genes (64.07% of the total protein-coding genes) and 1618 genes (26.4% of the total protein-coding genes) were identified as differentially expressed genes (abs (log2 fold change) ≥ 1) in the transcriptomic and proteomic analyses, respectively. Figure 1 shows the genome-wide multilayered omics results (genomics, transcriptomics, and proteomics) of *Delftia* sp. K82.

Characterization of the aniline degradation pathway of *Delftia* sp. K82 at the level of multi-omics analysis

According to the genomic analysis of *Delftia* sp. K82, *Delftia* sp. K82 had two different aniline degradation pathways (intradiol cleavage and extradiol cleavage). In a previous study, we suggested that *Delftia* sp. K82 induced two cleavage activities and reported a partial amino acid sequence of two pathway enzymes (Yun et al. 2004). However, we could not confirm the complete gene information of aniline degradation pathways because of the lack of a whole-genome sequence. Therefore, the whole genome sequence of *Delftia* sp. K82 was constructed in this study and the aniline degradation cluster was identified in the genome sequence. As a result, two complete aniline degradation pathways were obtained (Fig. 2). Their transcriptomic and proteomic induction levels are summarized in Table 3. The aniline oxygenase complex of *Delftia* sp. K82 (Nos. 1~6), converting aniline into catechol, and the extradiol cleavage pathway (Nos. 7~14) were highly induced more than 2-fold change in aniline condition at the transcriptional and translational levels (Table 3). However, induction of the intradiol cleavage pathway (Nos. 1-2~1-6), except for catechol 1,2-dioxygenase (No. 1-1) was less than 2-fold change or down-expressed in aniline condition. From these results, it was assumed that the extradiol cleavage of aniline was a major metabolic pathway. However, the role of the intradiol cleavage pathway of *Delftia* sp. K82 was not clear, but it seems to be complementary in the utilization of aniline.

Genome-wide characterization of aniline-induced high-copy metabolic enzymes of *Delftia* sp. K82

Semi-quantitative data of the whole proteome were obtained through spectral counts or mol% calculation using LC-MS/MS analysis (Ishihama et al. 2005). These data will be valuable for understanding the cell-based physiological status of bacteria at the proteomic level. For this purpose, 276 highly abundant proteins were selected from *Delftia* sp. K82 (90th percentile of mol%) for this analysis (Supplementary data 1). These abundant proteins were estimated to be approximately 71.5% of the total amount of whole proteins. For *Delftia* sp. K82 cultured in aniline, amount of proteins expression of 14 aniline degradation enzymes composed up to 11.9% of all proteins. Compared to *Delftia* sp. K82 cultured in LB

(less than 0.17% aniline degradation enzymes), the induction of aniline degradation enzymes was very tightly regulated in the presence of aniline in the culture media. However, significant variation in other basic metabolic enzymes, such as the tricarboxylic acid cycle, protein synthesis, and amino acid metabolism, were not identified (Fig. 3). This result indicated that *Delftia* sp. K82 makes essential metabolic enzymes regardless of the nutrition source provided. However, there were several upregulated abundant proteins in the aniline culture (Table 4).

Genome-wide characterization of aniline-induced cell wall and membrane proteins of *Delftia* sp. K82

Cell wall or membrane proteins play important roles in transport, signal transduction, and protection against extracellular stress (Park et al. 2012; Yun et al. 2011a). In the case of *Delftia* sp. K82, identification of aniline-induced cell wall and membrane proteins was important to elucidate the biodegradation activities of *Delftia* sp. K82. PSORTb was used to predict the subcellular location of induced proteins (Yu et al. 2010). Among the 95 proteins belonging to the cell wall and membrane fraction of the 276 highly abundant proteins of *Delftia* sp. K82, 12 proteins were identified that were significantly induced in aniline media (Table 4). Specifically, it is possible that porins (KDK82-RS00485) and transporters (KDK82-RS27635, RS31055, RS22955, RS00520, and RS01045) could be related to the transport of aniline or related metabolites. However, to fully understand the upregulated cell wall or membrane proteins, further functional studies, such as targeted mutagenesis, are required.

Conclusions

Multi-omics analysis of *Delftia* sp. K82 was performed, and it revealed the genome-wide response of *Delftia* sp. K82 to aniline. Both enzymes of the aniline degradation pathway and also aniline-induced novel proteins were identified. These results suggest that multi-omics approaches are useful tools for screening novel genes for a biodegradation response (Horinouchi et al. 2018; Yang et al. 2016). In particular, this approach can be applied to the elucidation of bacteria with diverse activities for organic compounds and the identification of novel enzymes for biodegradation (Swanson 1999). These enzymes can be used for the production of high-value added metabolites, which are used as precursors for biotechnological or pharmaceutical products (Hegazy et al. 2015; Zaks 2001).

Table 4 Upregulated abundant proteins in aniline culture condition except aniline degradation pathway

Locus_tag	Product	Localization	log2 Fold change	mol%	
			(ANI/LB)	LB	ANI
KDK82_RS01055	3-Oxoadipyl-CoA thiolase	Cytoplasmic	3.569	0.0287	0.3406
KDK82_RS28665	Succinate dehydrogenase iron-sulfur subunit	Cytoplasmic	1.735	0.0717	0.2386
KDK82_RS31120	Hypothetical protein	Cytoplasmic	6.663	0.0023	0.233
KDK82_RS06005	D-threitol dehydrogenase	Cytoplasmic	2.414	0.0398	0.2121
KDK82_RS00570	DUF1338 domain-containing protein	Cytoplasmic	5.790	0.0034	0.1881
KDK82_RS31100	Heme-binding protein	Cytoplasmic	6.047	0.0027	0.1785
KDK82_RS14040	Copper chaperone PCu(A)C	Cytoplasmic	2.310	0.0196	0.0972
KDK82_RS05985	Dihydroxyacetone kinase subunit L	Cytoplasmic	1.396	0.0348	0.0916
KDK82_RS00635	Aldehyde dehydrogenase	Cytoplasmic	1.916	0.0226	0.0853
KDK82_RS09610	Hcp1 family type VI secretion system effector	Extracellular	2.397	0.0431	0.227
KDK82_RS00485	Porin	Outer membrane	3.116	0.028	0.2428
KDK82_RS08655	TonB-dependent receptor	Outer membrane	5.814	0.0033	0.1857
KDK82_RS27635	Branched-chain amino acid ABC transporter substrate-binding protein	Periplasmic	1.287	0.1332	0.325
KDK82_RS31055	Tripartite tricarboxylate transporter substrate binding protein	Periplasmic	5.049	0.0088	0.2914
KDK82_RS22955	Tripartite tricarboxylate transporter substrate binding protein	Periplasmic	7.762	0.0011	0.2387
KDK82_RS31125	DcaA2	Periplasmic	3.552	0.017	0.1994
KDK82_RS03245	NADP-specific glutamate dehydrogenase	Periplasmic	2.153	0.0234	0.1041
KDK82_RS00520	Amino acid ABC transporter substrate-binding protein	Periplasmic	6.395	0.0012	0.101
KDK82_RS01045	Tripartite tricarboxylate transporter substrate binding protein	Periplasmic	3.015	0.0122	0.0986
KDK82_RS04080	DUF1993 domain-containing protein	Periplasmic	1.333	0.0375	0.0945
KDK82_RS20410	C4-dicarboxylate ABC transporter	Periplasmic	2.248	0.0173	0.0822

Supplementary Information

The online version contains supplementary material available at https://doi.org/10.1186/s40543-021-00258-6.

Additional file 1: Supplementary Table 1. High abundant proteins (90th percentile of mol%) in aniline culture condition of Delftia sp. K82.

Abbreviations

MAH: Mono aromatic hydrocarbon; LC-MS/MS: Liquid chromatography–mass spectrometry; LB: Luria-Bertani; PSORTb: Protein subcellular localization predictions; RSSR: Rapid Annotation using Subsystem Technology; COG: Clusters of orthologous group; DEG: Differentially expressed gene; DEP: Differentially expressed protein; CRISPER: Clustered regularly interspaced short palindromic repeats

Acknowledgements

Not applicable.

Availability of supporting data

Research data have been provided in the manuscript.

Authors' contributions

SIK and SYL performed data analysis. HYL, GWS, and SHY carried out all experimental work. SIK designed and wrote the manuscript. All authors read and approved the final manuscript.

Funding

This work was supported by the Korea Basic Science Institute research program (No. C030130 and C030222), and the National Research Foundation of Korea (NRF) grant funded by the Korea government (MSIT) (No. 2020R1C1C1009941).

Competing interests

The authors declare that they have no competing interests.

Author details

[1]Research Center for Bioconvergence Analysis, Korea Basic Science Institute, Ochang 28119, South Korea. [2]Center for Research Equipment, Korea Basic Science Institute, Ochang 28119, South Korea. [3]Department of Bio-Analytical Science, University of Science and Technology (UST), Daejeon 34113, Korea.

Received: 6 October 2020 Accepted: 13 January 2021
Published online: 05 February 2021

References

Almagro Armenteros JJ, Tsirigos KD, Sonderby CK, et al. SignalP 5.0 improves signal peptide predictions using deep neural networks. Nat Briotechnol. 2019;37(4):420–3. https://doi.org/10.1038/s41587-019-0036-z.

Anders S, Pyl PT, Huber W. HTSeq—a Python framework to work with high-throughput sequencing data. Bioinformatics. 2015;31(2):166–9. https://doi.org/10.1093/bioinformatics/btu638.

Aziz RK, Bartels D, Best AA, et al. The RAST Server: rapid annotations using subsystems technology. BMC Genomics. 2008;9:75. https://doi.org/10.1186/1471-2164-9-75.

Bolger AM, Lohse M, Usadel B. Trimmomatic: a flexible trimmer for Illumina sequence data. Bioinformatics. 2014;30(15):2114–20. https://doi.org/10.1093/bioinformatics/btu170.

Chan PP, Lowe TM. tRNAscan-SE: searching for tRNA genes in genomic sequences. Methods Mol Biol. 2019;1962:1–14. https://doi.org/10.1007/978-1-4939-9173-0_1.

Chen Y, Yu P, Luo J, Jiang Y. Secreted protein prediction system combining CJ-SPHMM, TMHMM, and PSORT. Mammalian Genome. 2003;14(12):859–65. https://doi.org/10.1007/s00335-003-2296-6.

Dobin A, Davis CA, Schlesinger F, et al. STAR: ultrafast universal RNA-seq aligner. Bioinformatics. 2013;29(1):15–21. https://doi.org/10.1093/bioinformatics/bts635.

Feng Y, Chen LL, Zhang T, Wu YH, Song L, Wang Y. Research progress on health effects of aniline. Zhonghua Yu Fang Yi Xue Za Zhi. 2020;54(2):213–8. https://doi.org/10.3760/cma.j.issn.0253-9624.2020.02.019.

Fuchs G, Boll M, Heider J. Microbial degradation of aromatic compounds—from one strategy to four. Nat Rev Microbiol. 2011;9(11):803–16. https://doi.org/10.1038/nrmicro2652.

Grant JR, Stothard P. The CGView Server: a comparative genomics tool for circular genomes. Nucleic Acids Res. 2008;36(Web Server issue):W181–4. https://doi.org/10.1093/nar/gkn179.

Grissa I, Vergnaud G, Pourcel C. CRISPRFinder: a web tool to identify clustered regularly interspaced short palindromic repeats. Nucleic Acids Res. 2017;35(Web Server issue):W52–57. https://doi.org/10.1093/nar/gkm360.

Hegazy ME, Mohamed TA, ElShamy AI, et al. Microbial biotransformation as a tool for drug development based on natural products from mevalonic acid pathway: a review. J Adv Res. 2015;6(1):17–33. https://doi.org/10.1016/j.jare.2014.11.009.

Horinouchi T, Maeda T, Furusawa C. Understanding and engineering alcohol-tolerant bacteria using OMICS technology. World J Microbiol Biotechnol. 2018;34(11):157. https://doi.org/10.1007/s11274-018-2542-4.

Ishihama Y, Oda Y, Tabata T, et al. Exponentially modified protein abundance index (emPAI) for estimation of absolute protein amount in proteomics by the number of sequenced peptides per protein. Mol Cell Proteomics. 2005;4(9):1265–72. https://doi.org/10.1074/mcp.M500061-MCP200.

Lagesen K, Hallin P, Rodland EA, Staerfeldt HH, Rognes T, Ussery DW. RNAmmer: consistent and rapid annotation of ribosomal RNA genes. Nucleic Acids Res. 2007;35(9):3100–8. https://doi.org/10.1093/nar/gkm160.

Lee SY, Kim GH, Yun SH, et al. Proteogenomic characterization of monocyclic aromatic hydrocarbon degradation pathways in the aniline-degrading bacterium burkholderia sp. K24. PloS One. 2016;11(4):e0154233. https://doi.org/10.1371/journal.pone.0154233.

Liu Z, Yang H, Huang Z, Zhou P, Liu SJ. Degradation of aniline by newly isolated, extremely aniline-tolerant Delftia sp. AN3. Appl Microbiol Biotechnol. 2002;58(5):679–82. https://doi.org/10.1007/s00253-002-0933-8.

Love MI, Huber W, Anders S. Moderated estimation of fold change and dispersion for RNA-seq data with DESeq2. Genome Biol. 2014;15(12):550. https://doi.org/10.1186/s13059-014-0550-8.

Park JS, Lee WC, Yeo KJ, et al. Mechanism of anchoring of OmpA protein to the cell wall peptidoglycan of the gram-negative bacterial outer membrane. FASEB J. 2012;26(1):219–28. https://doi.org/10.1096/fj.11-188425.

Schmieder R, Edwards R. Quality control and preprocessing of metagenomic datasets. Bioinformatics. 2011;27(6):863–4. https://doi.org/10.1093/bioinformatics/btr026.

Seemann T. Prokka: rapid prokaryotic genome annotation. Bioinformatics. 2014;30(14):2068–9. https://doi.org/10.1093/bioinformatics/btu153.

Swanson PE. Dehalogenases applied to industrial-scale biocatalysis. Curr Opin Biotechnol. 1999;10(4):365–9. https://doi.org/10.1016/S0958-1669(99)80066-4.

Yang FC, Chen YL, Tang SL, et al. Integrated multi-omics analyses reveal the biochemical mechanisms and phylogenetic relevance of anaerobic androgen biodegradation in the environment. ISME J. 2016;10(8):1967–83. https://doi.org/10.1038/ismej.2015.255.

Yu NY, Wagner JR, Laird MR, et al. PSORTb 3.0: improved protein subcellular localization prediction with refined localization subcategories and predictive capabilities for all prokaryotes. Bioinformatics. 2010;26(13):1608–15. https://doi.org/10.1093/bioinformatics/btq249.

Yun SH, Choi CW, Kwon SO, et al. Quantitative proteomic analysis of cell wall and plasma membrane fractions from multidrug-resistant Acinetobacter baumannii. J Proteome Res. 2011a;10(2):459–69. https://doi.org/10.1021/pr101012s.

Yun SH, Park GW, Kim JY, et al. Proteomic characterization of the Pseudomonas putida KT2440 global response to a monocyclic aromatic compound by iTRAQ analysis and 1DE-MudPIT. J Proteomics. 2011b;74(5):620–8. https://doi.org/10.1016/j.jprot.2011.01.020.

Yun SH, Yun CY, Kim SI. Characterization of protocatechuate 4,5-dioxygenase induced from p-hydroxybenzoate-cultured Pseudomonas sp. K82. J Microbiol. 2004;42(2):152–5.

Zaks A. Industrial biocatalysis. Curr Opin Chem Biol. 2001;5(2):130–6. https://doi.org/10.1016/s1367-5931(00)00181-2.

Publisher's Note